Atmospheric
Chemistry
and Physics
Discussions

Open Access

Secondary organic aerosol formation during June 2010 in Central Europe: measurements and modelling studies with a mixed thermodynamic-kinetic approach

B. Langmann[1], K. Sellegri[2], and E. Freney[2]

[1]Institute of Geophysics, University of Hamburg, KlimaCampus, Hamburg, Germany
[2]Laboratoire de Meteorologie Physique, CNRS, Universite Blaise Pascal Aubiere, France

Correspondence to: B. Langmann (baerbel.langmann@zmaw.de)

ACPD

13, 26761–26793, 2013

Secondary organic aerosol formation during June 2010 in Central Europe

B. Langmann et al.

Title Page

Abstract	Introduction
Conclusions	References
Tables	Figures

◄◄ ►►

◄ ►

Back Close

Full Screen / Esc

Printer-friendly Version

Interactive Discussion

Secondary organic aerosol formation during June 2010 in Central Europe

B. Langmann et al.

Title Page

Abstract	Introduction
Conclusions	References
Tables	Figures

|◄ | ►|

◄ | ►

Back | Close

Full Screen / Esc

Printer-friendly Version

Interactive Discussion

Abstract

Until recently secondary organic carbon (SOC) aerosol mass concentrations have been systematically underestimated by three-dimensional atmospheric-chemistry-aerosol models. With a newly proposed concept of aging of organic vapours more realistic model results for organic carbon aerosol mass concentrations could be achieved. Applying a mixed thermodynamic-kinetic approach for SOC aerosol formation shifted the aerosol size distribution towards particles in the cloud condensation nuclei size range, thereby emphasising the importance of SOC aerosol formation schemes for modelling realistic cloud and precipitation formation. The additional importance of hetero-molecular nucleation between H_2SO_4 and organic vapours remains to be evaluated in three-dimensional atmospheric-chemistry-aerosol models. Here a case study is presented focusing on Puy-de-Dôme, France in June 2010. Even though nucleation events at Puy-de-Dôme were rare during the chosen period of investigation a weak event in the boundary layer could be reproduced by the model when nucleation of low-volatile secondary organic vapour is included. Differences in the model results with and without nucleation of organic vapour are visible in the lower free troposphere over several days of the period. Taking into account nucleation of organic vapour leads to an increase in accumulation mode particles due to coagulation of nucleation and aitken mode particles. Moreover, the measurements indicate a considerable increase in SOC aerosol mass concentration during the measurement campaign, which could be reproduced by modelling using a simplified thermodynamic-kinetic approach for SOC aerosol formation and increased biogenic VOC precursor emissions. Comparison with a thermodynamic SOC aerosol formation approach shows a huge improvement in modelled SOC aerosol mass concentration with the thermodynamic-kinetic approach for SOC aerosol formation and a slight improvement of modelled particle size distribution.

1 Introduction

Measurements of the chemical composition of atmospheric aerosol indicate a contribution of organic carbon (OC) ranging from 20 to 70 % to the submicron particulate matter mass (Jimenez et al., 2009). Primary organic carbon (POC) aerosols are directly emitted into the atmosphere whereas secondary organic carbon (SOC) aerosols are formed by atmospheric oxidation of organic vapours (here called secondary organic gases: SOG). SOC makes up between 36 and 80 % of the total OC concentration of atmospheric aerosol worldwide (Jimenez et al., 2009). Until recently, atmospheric models systematically underestimated measured OC aerosol mass concentrations in the atmosphere by a factor of up to 10 and more (e.g. Heald et al., 2005; Jimenez et al., 2009; Yu, 2011). This underestimation is partly due to a lack of understanding of SOC aerosol formation mechanisms with the large number of different organic compounds involved (e.g. Griffin et al., 2002; Kroll and Seinfeld, 2008; Halquist et al., 2009), and has hindered an adequate implementation into three-dimensional atmospheric-chemistry-aerosol models until today.

In contrast to SOC aerosol formation, sulfate formation takes place through oxidation of SO_2 followed by either irreversible condensation of sulphuric acid molecules on pre-existing particles or nucleation to form new particles. The formation of SOC aerosol is much more complex due to the semi-volatile nature of the precursor gas-phase species and the enormous number of different organic compounds involved. The widely used thermodynamic two product approach of gas-particle partitioning between semi-volatile OC compounds in the gas-phase and the aerosol phase according to Henry's law (Pankow, 1994; Odum et al., 1996) was found to be insufficient in reproducing measured SOC aerosol concentrations (Yu, 2011). Taking into account more precursor gases, e.g. isoprene (e.g. Henze and Seinfeld, 2006) increase modelled SOC aerosol mass concentrations, but the general underestimation remains. As already pointed out by Heald et al. (2005) and references therein, successive generation of oxidation products following the first stage of oxidation of emitted hydrocarbons

may increase the condensable amount of organic vapours thereby producing higher SOC aerosol mass concentrations. Jimenez et al. (2009) proposed the concept of aging of organic vapours, thereby producing less volatile and higher oxygenated organic vapours which can generate atmospheric SOC aerosol mass concentrations comparable to sulfate. Based on these ideas several recent studies have considered the aging of organic vapours and/or aerosols based on thermodynamic partitioning (e.g. Hodzic et al., 2010; Shivastava et al., 2011; Bergstroem et al., 2012). Yu (2011) developed another promising modelling strategy for the formation of SOC aerosols considering the aging of SOG. In addition to the traditional two compound thermodynamic gas-particle partitioning, a third low volatile organic compound (LV-SOG) is introduced, which kinetically undergoes condensation on pre-existing particles. This is a major difference to the widely applied thermodynamic approaches. It was shown that modelled annual mean SOC aerosol mass concentrations increased by a factor of 2–20 in many parts of the boundary layer worldwide (Yu, 2011). In addition, the modelled aerosol size distribution shifted from particles less than 10 nm to those of the size of cloud condensation nuclei (about 50–100 nm). This highlights the importance of reliable SOC aerosol formation mechanism for more realistic model simulation results concerning clouds and precipitation formation.

Furthermore, the role of low volatile organic vapours in new particle formation in addition to H_2SO_4 nucleation has received increasing attention in recent years. It has been demonstrated that H_2SO_4 nucleation alone cannot always adequately explain observed particle number concentrations and size distributions (e.g. Fiedler et al., 2005; Hamed et al., 2010; Kerminen et al., 2010; Metzger et al., 2010; Paasonen et al., 2010). To our knowledge, three-dimensional modelling studies on SOG nucleation are not yet available.

Based on the approach developed by Yu (2011) we extended the SOC aerosol formation mechanism of the regional three-dimensional atmosphere-chemistry-aerosol model REMOTE (Langmann et al., 2008; Anttila et al., 2010). We implemented even more generalised assumptions than Yu (2011) for easy use in regional or global CTM's

or on-line atmosphere-chemistry-aerosol models. Different to Yu (2011) we consider also the contribution of anthropogenic SOG to SOC aerosol formation and include the nucleation of low-volatile SOG. The model set-up and the SOC aerosol formation scheme are described in Sect. 2. Section 3 describes a measurement campaign at Puy-de-Dôme, France in June 2010, which provides a set of measurements used to evaluate the model results presented in Sect. 4. The last section provides conclusions and an outlook.

2 Model description

2.1 Model set-up

We use the regional three-dimensional on-line climate-chemistry-aerosol model RE-MOTE (Regional Model with Tracer Extension) (Langmann, 2000; Langmann et al., 2008). REMOTE has been developed and applied to understand the dispersion and photochemical transformation of anthropogenic and natural gaseous and aerosol emissions (e.g. Langmann et al., 2003, 2008). The dynamical part of the model is based on the former regional weather forecast system of the German Weather Service (Majewski, 1991), which is using a hydrostatic assumption for the vertical pressure gradient. In addition to the German Weather Service physical parameterisations, those of the global climate model ECHAM-4 (Roeckner et al., 1996) have been implemented in REMOTE and are used for the current study.

The domain is subdivided into 81×91 grid boxes of $0.5°$ resolution (approximately 55 km) on a rotated latitude/longitude grid with 19 vertical layers of increasing thickness between the Earth's surface and the 10 hPa pressure level using terrain following hybrid pressure-sigma coordinates. A model time step of 5 min is chosen. REMOTE is initialised using meteorological analysis data of the European Centre for Medium Range Weather Forecast (ECMWF), which are updated at the lateral model boundaries every 6 h with linear interpolation in between. Every 30 h, ECMWF data are used

for an update over the whole model domain to force the model to stay close to the observed weather situation. The prognostic equations for surface pressure, temperature, specific humidity, cloud water, horizontal wind components and aerosol mass mixing ratios are written on an Arakawa-C grid.

For the determination of aerosol dynamics and thermodynamics we use the M7 module, which is described in detail in Vignati et al. (2004) and Langmann et al. (2008). The aerosol dynamical processes in the standard M7 include nucleation, coagulation and condensation. The five aerosol components considered in the standard M7 are sulfate, black carbon, organic carbon, sea salt and mineral dust. For the current application of the REMOTE model over Europe, mineral dust is not considered. The aerosol size spectrum is represented by the superposition of seven log-normal distributions subdivided into a soluble and an insoluble coarse, accumulation and aitken mode and an additional soluble nucleation mode. Photochemical production and loss in REMOTE is determined by the RADM II chemical scheme (Stockwell et al., 1990) including a wide range of hydrocarbon degradation reactions. Photolysis rates are calculated based on Madronich (1987). Aqueous phase chemistry processes is implemented according to Walcek and Taylor (1986).

After being released in the atmosphere, gas phase and aerosol phase species undergo transport processes (horizontal and vertical advection, Smolarkiewitz, 1983, transport in convective clouds (Tiedtke, 1989), vertical turbulent diffusion (Mellor and Yamada, 1974)) and are removed from the atmosphere by sedimentation, dry and wet deposition. Dry deposition fluxes for gaseous compounds are determined after Wesley (1989). For aerosol particles, the same size-dependent parameterisations as in the ECHAM5-HAM model (Stier et al., 2005) are used for dry deposition and sedimentation. Wet deposition is computed according to Walcek and Taylor (1986) by integrating the product of the grid-averaged precipitation rate and the mean cloud water concentration which is determined from cloud base (first layer above the surface containing more than $0.001\,\mathrm{g\,kg^{-1}}$ liquid water) to cloud top (highest level exceeding an amount of $0.001\,\mathrm{g\,kg^{-1}}$ liquid water) for fair weather clouds and from the surface to cloud top

Title Page

Abstract | Introduction

Conclusions | References

Tables | Figures

◄ | ►►

◄ | ►

Back | Close

Full Screen / Esc

Printer-friendly Version

Interactive Discussion

for raining clouds. Scavenging efficiencies are based on Kasper-Giebl et al. (2000) distinguishing between soluble and insoluble aerosols dependent on cloud liquid water content. Size dependent scavenging has not been taken into account until now. In-cloud produced sulfate is distributed to the available pre-existing accumulation and coarse mode aerosol particles according to the respective number concentration (Stier et al., 2005).

2.2 SOC aerosol formation scheme

The standard M7 aerosol scheme (Vignati et al., 2004) has been extended by Anttila et al. (2010) by a thermodynamic two compound SOC aerosol formation mechanism to consider isoprene oxidation products for SOC formation. In accordance with the M7 aerosol scheme described above, the two SOC aerosol components (medium- and semi-volatile SOC) may be formed in the soluble aitken, accumulation and coarse mode so that in total six new aerosol tracers have been implemented by Antilla et al. (2010). We extended the SOC formation scheme of Antilla et al. (2010) from the pure thermodynamic approach to a mixed thermodynamic-kinetic one including aging of SOG (Fig. 1) based on Yu (2011).

For the formation of medium- and semi-volatile SOG (MV-SOG and SV-SOG) we consider all chemical reactions of hydrocarbons and oxygenated hydrocarbons (e.g. acetaldehyde) with OH, NO_3 and O_3 of the RADM-II photochemical mechanism (Stockwell et al., 1990). The formation of MV-SOG and SV-SOG is determined according to the prescribed yields and Henry Law constants (Table 1, modified from Anttila et al., 2010) based on physico-chemical properties of 1,3-propanediol for MV-SOG and 1,2,4-butenetriol for SV-SOG (Saxena and Hildemann, 1996).

We consider aging of the MV-SOG to SV-SOG and further aging of SV-SOG to low-volatile SOG (LV-SOG), with the latter compound being newly introduced into REMOTE. Aging is assumed to occur via OH-oxidation with $k = 3 \times 10^{11}$ cm^3 molecules^{-1} s^{-1} according to Jimenez et al. (2009). Like in Yu (2011) the loss of OH radicals by oxidation aging of SOG is ignored. To further simplify the approach

of Yu (2011) we determine the mass-conserving transformation rate of MV-SOG → SV-SOG and SV-SOG → LV-SOG by prescribing a maximum threshold of the reactant concentration being available for oxidation. This way we avoid determining the saturation vapour pressure of the oxidised SOG compounds, which greatly simplifies the procedure proposed by Yu (2011). Results with 1 % and 10 % threshold values (in the latter case an additional requirement is that OH concentrations exceed 0.1 ppt thereby excluding night-time aging processes) are presented in Sect. 4.2. The quasi steady-state assumption for SOG oxidation as applied in Anttila et al. (2010) is no longer valid when oxidation aging is considered. Therefore, in the current version the three SOG components are also subject of transport and removal processes.

LV-SOG is assumed to condense kinetically on pre-existing particles while for MV-SOG and SV-SOG the thermodynamic partitioning approach of Anttila et al. (2010) is used as shown in Fig. 1. In addition, nucleation of LV-SOG is considered, so that in total four new LV-SOC components have been added to the model. In a first step, LV-SOG nucleation and kinetic condensation is treated in the same way as H_2SO_4 in the M7 module (Stier et al., 2005; Vignati et al., 2004). As condensation on pre-existing particles and nucleation of new particles compete for the available LV-SOG, first the maximum amount of condensable LV-SOG on pre-existing particles is calculated. The remaining LV-SOG is available for the nucleation of new clusters. The number of nucleated particles and the mass of nucleated LV-SOG is determined using the homogeneous nucleation parameterisation of Vehkamaeki et al. (2002).

2.3 Emissions

Anthropogenic emissions of SO_x, NO_x, NH_3, CO, VOCs and $PM_{2.5}$ obtained from the EMEP emission inventory (http://www.ceip.at/) are prescribed as monthly fluxes as described in Marmer and Langmann (2007). In addition to anthropogenic emissions, terrestrial biogenic terpene and isoprene emissions from forests are considered based on Guenther et al. (1991, 1993). Marine POC emissions are determined following O'Dowd et al. (2008) and Gantt et al. (2011). Further details of the treatment of primary anthro-

B. Langmann et al.

Title Page

Abstract	Introduction
Conclusions	References
Tables	Figures

◄◄　　　►►

◄　　　►

Back　　Close

Full Screen / Esc

Printer-friendly Version

Interactive Discussion

pogenic aerosol emissions and marine sea-spray emissions are described in Lang-
mann et al. (2008).

3   Measurement campaign

During June 2010 a two weeks intensive measurement campaign (21 June–4 July)
took place at Puy-de-Dôme, France approximately 10 km away from Clermont-Ferrand.
Puy-de-Dôme (45°46′ N 02°57′ E; 1464 m a.s.l.) is a large lava dome and one of the
youngest volcanoes in the Chaîne des Puys region of Massif Central in south-central
France.

The principle goals of the measurement campaign were to evaluate aerosol size
distribution and chemistry in the boundary layer and lower free troposphere but also
to characterise aerosol early growth dynamics during new particle formation events at
high altitude. In addition to a number of online and offline instrumentation, aerosol size
distribution was measured using a scanning mobility particle sizer (SMPS), selecting
particles diameters between 30 nm and 500 nm with a time resolution of 120 s. Aerosol
chemical composition and mass concentration of the non-refractory submicron partic-
ulate matter was measured with an Aerodyne Time-of-Flight Aerosol Mass Spectrome-
ter (C-ToF-AMS) (Drewnick et al., 2005; Cangaratna et al., 2007). The C-ToF-AMS was
sampling behind a whole air inlet during the cloud free period after 22 June. During 20–
22 June, when cloudy conditions prevail at Puy-de-Dôme, C-ToF-AMS was sampling
behind an interstitial inlet. More detailed description of the C-ToF-AMS set-up and re-
sults during measurement campaigns in 2008, 2009 and 2010 are available in Freney
et al. (2011). The resolved mass concentrations include ammonium, sulfate, nitrate,
organic carbon and chloride species. In order to extract chemically resolved mass con-
centrations of individual aerosol species, the AMS raw data are evaluated with standard
assumptions as described by Allan et al. (2004). The organic carbon aerosol mass con-
tributed up to 56 % to the total aerosol mass and increased gradually with temperature.

Title Page

Abstract | Introduction

Conclusions | References

Tables | Figures

◄ | ►◄

◄ | ►

Back | Close

Full Screen / Esc

Printer-friendly Version

Interactive Discussion

Positive matrix factorisation analysis of the organic aerosol separated a low volatility oxidised organic aerosol.

4   Model results and comparison with observations

4.1   Meteorological conditions

The week before the two weeks intensive measurement campaign (21 June–4 July) at Puy-de-Dôme, France was characterised by heavy rainfall events and day-time temperatures well below 20 °C in many parts of western Europe. The coldest day was the mid-summer day where even freezing at ground level was measured locally. During the first measurement campaign week, temperatures increased all over Europe due to the build-up of a high-pressure system, which lasted until the end of the measurement campaign in early July 2010. Precipitation was not measured in the Puy-de-Dôme area after 20 June, whereas the model determines small amounts of precipitation on 24 June and a convective precipitation event on 28/29 June. In this context it should be considered, that model results are produced in 0.5° resolution, thereby representing average conditions for a larger area than Puy-de-Dôme alone. Measured and modelled temperature and relative humidity at Puy-de-Dôme during June 2010 are displayed in Fig. 2. Model results are shown for the first and second model layer. This is done because the measurement location with the peak of Puy-de-Dôme is not resolved by the model's horizontal resolution of 0.5°. In the following sections, model simulation results focussing on the first model layer will be presented. Altogether, REMOTE model simulation results during June 2010 around Puy-de-Dôme reproduce satisfactory the observed meteorological situation.

Title Page

Abstract   Introduction

Conclusions   References

Tables   Figures

◀◀   ▶▶

◀   ▶

Back   Close

Full Screen / Esc

Printer-friendly Version

Interactive Discussion

4.2 Atmospheric aerosol concentrations

4.2.1 Aerosol mass concentration

Sulfate and chlorine aerosol mass concentrations at Puy-de-Dôme are well captured in the model simulation results (Fig. 3), although sulphate concentrations are gener-
⁵ ally underestimated. Sulfate formation is limited by the availability of oxidants, rather than SO_2 and is therefore in competition with other oxidation processes. For chloride, only the modelled accumulation mode concentration is displayed in Fig. 3, as AMS does not capture coarse mode particles. Modelled chloride mass concentrations in-cluding coarse and accumulation mode chloride reaches maximum concentration up
¹⁰ to 17 µg m^{-3} on 22 June. These peak concentrations are connected to the transport of marine air masses, which is reported to contribute to Puy-de-Dôme about one quarter of time during summer (Venzac et al., 2009). It should be emphasised again that the AMS measurements on 20–22 June were made under cloudy conditions behind an in-terstitial inlet (see Sect. 3) restricting the sampling in comparison to the whole air inlet,
¹⁵ which was used during the following campaign days. In addition, submicron chloride originating from sea salt is only partially detected by the AMS due to its high volatilisa-tion temperature, but the exact fraction is not known for the measurements presented here (Ovadnevaite et al., 2012).

The measured organic carbon aerosol mass concentration is shown in Fig. 4 (dark
²⁰ blue line). In order to illustrate the sensitivity of OC model results on SOC aerosol parameterisations, Fig. 4 shows the results for the original two compound thermody-namic approach for isoprene only by Anttila et al. (2010) (grey line) and model results with additional VOC precursor gases (yellow line). Although a slight increase in OC mass concentration takes place, the model results are still far below the measure-
²⁵ ments. Taking into account SOG as additional prognostic trace species in the model, which undergoes transport and removal (green line) leads to a slight and still insuffi-cient increase in comparison with the measurements. This holds also for a sensitivity study where in addition to transport and removal of SOG, biogenic VOC emissions are

Title Page

Abstract	Introduction
Conclusions	References
Tables	Figures

⏮   ⏭

◀   ▶

Back   Close

Full Screen / Esc

Printer-friendly Version

Interactive Discussion

increased by a factor of 5 due to their overall uncertainty (orange line). The red line in Fig. 4 shows results from the simulation where aging of MV-SOG to SV-SOG has been considered, generating OC aerosol mass concentrations approaching the measurements. Taking into account the aging of SV-SOG to LV-SOC (second aging step, black line) does not modify OC aerosol mass concentrations much in comparison to the first aging step. A further slight increase in OC aerosol mass concentration is achieved by assuming 10 % (light blue line in Fig. 4) instead of 1 % of aging (see Sect. 2.2). Increasing the amount of biogenic VOC emissions by a factor of 5 in the 10 % aging simulation leads to a considerable increase in OC aerosol mass concentrations in the range of the measurements. SOC mass concentration remains nearly unchanged taking into account nucleation of LV-SOC. The reasons lie in the absence of nucleation events in the boundary layer during the high pressure period. Further discussion on the role of SOC nucleation is presented in Sect. 4.3.2.

The reduction of modelled OC mass concentration on 24 June is connected to small amounts of modelled stratiform precipitation. Similarly, the modelled OC mass concentration is reduced again on 28/29 June as a result of a convective precipitation event determined by the model. The increase of SOC concentrations throughout the high pressure period was not restricted to Puy-de-Dôme but took place over large parts of Europe (Fig. 5) with concentrations greatly exceeding $5 \, \mu g \, m^{-3}$. A diurnal cycle in observed OC concentration is nearly invisible.

Applying different thresholds for the available SOG for aging, e.g. 1 % or 10 %, respectively, modified the amount of semi-volatile SOC (note, that here the sum of modelled MV-SOC and SV-SOC is meant) and LV-SOC considerably (Fig. 6). Assuming 1 % of aging overestimates the amount of semi-volatile SOC, which in this case consists mainly of MV-SOC. Due to the limited amount of SV-SOG, LV-SOC is greatly underestimated. Assuming 10 % of aging when OH concentrations exceeds 0.1 ppt leads to much better agreement between modelled and measured semi-volatile SOC and LVSOC. A further increase to 50 % aging shows no considerable effects.

To extend the evaluation of the applied SOC formation scheme, further model simulations over Europe for different periods (January 2003, June 2003) were conducted for comparisons with data presented in Langmann et al. (2008). During June 2003 a considerable improvement in modelled OC mass concentrations over Europe could be achieved with the SOC formation scheme described here (Supplement Fig. S1). However, during winter conditions in January 2003, improvements of model OC concentrations were not achieved, indicating further deficiencies. See Sect. 5 for more discussions.

4.2.2 Aerosol size distribution, number concentration and nucleation

Although SOC aerosol mass concentration remains nearly unchanged when taking into account the second aging step in addition to the first aging step (Fig. 4), it should be noted, that considerable differences in the aerosol size distribution are determined between these two model simulations and the pure thermodynamic approach. Figure 7 compares the modelled size distribution in the near surface fresh (20, 21 June) and aged (26, 27 June) air masses at Puy-de-Dôme for the pure thermodynamic approach (corresponding to the green line in Fig. 4) and for the first aging step (corresponding to the red line in Fig. 4, however with 10 % aging) against the mixed thermodynamic-kinetic approach (corresponding to the light blue line in Fig. 4). The measurements indicate a considerable increase in aerosol number concentration of accumulation mode particles from 20–27 June 2010 by more than $5000 \, \text{cm}^{-3}$ accompanied by a considerable decrease of aitken mode particles of about $7000 \, \text{cm}^{-3}$. It should be noted, however, that only interstitial particles were measured before 23 June (see Sect. 3). Considering that the model applies a modal approach for the size distribution, it can satisfactorily reproduce the measurements in the fresh air masses although the modelled absolute number concentration is smaller than the observed one. Aged air masses show a considerable increase in modelled particle number concentration of accumulation mode particles. Different to the observations, modelled aitken mode particle number concentration increases as well from 20–27 June. The reason is the emission of

Title Page

Abstract   Introduction

Conclusions   References

Tables   Figures

|◄   ►|

◄   ►

Back   Close

Full Screen / Esc

Printer-friendly Version

Interactive Discussion

primary OC and BC aerosols released into the insoluble aitken mode in the first model layer, which accumulates in the PBL (Planetary Boundary Layer), in particular in the surface layer during night-time. However, the Puy-de-Dôme measurement location is in the residual layer above the surface layer during night-time. Therefore, night-time data has been excluded from the model data analysis in Fig. 7. Nevertheless, an overestimation aitken mode particle number concentration remains. Again, it should be noticed here, that the model resolution of 0.5° is too coarse to catch the special conditions at Puy-de-Dôme exactly.

In the fresh air masses, the pure thermodynamic approach shows more particles in the aitken mode than the thermodynamic-kinetic approach, similar to Yu (2011). With the thermodynamic-kinetic approach a faster growth to accumulation mode particles takes place during the aging process. In the aged air masses, the differences are much smaller, however a determination of bigger particles remains with the thermodynamic-kinetic approach. Considering only the first aging step for SOC aerosol formation results in an increase of SV-SOG as further consumption for LV-SOG formation is excluded. Gas-particle partitioning of SV-SOG is the major reason for the shift in the mode radii. Due to the thermodynamic equilibrium assumptions, the irreversible growth of the aitken mode particles into the accumulation mode is not allowed in this case, so that accumulation mode particle number concentration increases at a slower rate during aging compared to the thermodynamic-kinetic approach. Generally, the thermodynamic-kinetic approach can more realistically reproduce the observed data than the pure thermodynamic approach, in particular in fresh air-masses.

Further comparison of near surface air masses all over Europe (Fig. 8) shows that the differences between the thermodynamic approach and the thermodynamic-kinetic approach are not restricted to Puy-de-Dôme, but occur over large areas of Europe. This confirms the analysis of Henne et al. (2010) that measurements at Puy-de-Dôme are generally representative for a larger area and therefore suitable for the evaluation of European scale models. In the lower free troposphere, however, the particle number concentrations determined by the thermodynamic-kinetic approach in the aitken

Title Page

Abstract | Introduction

Conclusions | References

Tables | Figures

◀ | ▶

◀ | ▶

Back | Close

Full Screen / Esc

Printer-friendly Version

Interactive Discussion

and accumulation mode remain slightly smaller than those calculated with the thermodynamic approach. The reason is that nucleation is of increasing importance with increasing height in the thermodynamic-kinetic approach, thereby generating more nucleation mode particles.

The chosen episode is unfortunately not suitable to study the role of LV-SOG nucleation, as nucleation events at Puy-de-Dôme were rare during the period of observation. Model simulation results with and without LV-SOG nucleation at Puy-de-Dôme are shown in Fig. 9. One nucleation event took place on 20 June, just before the intensive measurement campaign. This nucleation event was detected in the model results considering LV-SOG nucleation and in the measurements with SMPS. However, it was weak and without much implications, as precipitation reduces particle number concentrations considerably. Differences in the model results with and without LV-SOG nucleation are visible in the lower free troposphere over several days of the period, where due to coagulation of nucleation and aitken mode particles an increase of accumulation mode particles occurs when nucleation of LV-SOG is taken into account. Further studies will be necessary to illuminate the role of LV-SOG nucleation in the PBL and lower free troposphere and the role of this process for the formation of particles in the size range of CCN particles.

5 Conclusions and outlook

A considerable increase in modelled SOC aerosol mass concentration at Puy-de-Dôme, France as measured during an intensive observation campaign in June 2010 was achieved by taking into account aging processes of SOC precursor gases and thereby more realistically reproducing measured SOC aerosol concentrations. In contrast to the pure thermodynamic gas-particle partitioning approach usually applied for modelling SOC aerosol formation, we use a mixed thermodynamic-kinetic approach based on Yu (2011), which produced higher and more realistic SOC aerosol mass concentrations. Biogenic VOC precursor emissions play an important role. By using the

mixed thermodynamic-kinetic approach for SOC aerosol formation, their overall uncertainty offers an explanation for the differences in measured and modelled SOC aerosol mass concentration at Puy-de-Dôme. This does not hold for the pure thermodynamic SOC formation mechanism, where modelled SOC aerosol mass concentrations remain far below the measurements even when biogenic VOC emissions are increased. Compared to a pure thermodynamic SOC formation mechanism, an increase of aerosols in the size range of CCN during a period with multiple nucleation events in the PBL is reported by Yu (2011). During the period investigated here, nucleation events in the PBL were rare, but a considerable increase in accumulation mode particle number concentration were determined with the mixed kinetic-thermodynamic approach in comparison to the pure thermodynamic one, in particular in fresh air masses. These results emphasise the inter-relationship of reliable SOC formation mechanism and aerosol-cloud interactions for more realistic model simulation results concerning clouds and precipitation formation.

New developments considering hetero-molecular nucleation between H_2SO_4 and organic vapours have been published recently (Paasonen et al., 2010), but to our knowledge they have not yet been evaluated in three-dimensional atmosphere-chemistry-aerosol model simulations. Unfortunately, the period investigated here represents an unsuitable episode to investigate co-nucleation of H_2SO_4 and organic vapours in the PBL due to the rare nucleation events taking place. Therefore further model application will be necessary to illuminate the role of SOG nucleation.

In addition to aging processes of SOG and thermodynamic and kinetic SOC formation processes, other SOC formation processes are discussed in the literature, like SOC formation in the aqueous phase (Ervens et al., 2011) or new SOC particle formation on pre-existing ionised clusters (e.g. Zhang et al., 2011). For future investigations it is worth to consider that Puy-de-Dôme, located in the mountainous area of the Central Massif in France, is known as a region of higher 222-Rn surface concentration than the surrounding (Szegvary et al., 2009), thereby potentially offering a higher concentration of ionised clusters as sites for new SOC particle formation.

Similar to other past and recent modelling studies on OC aerosols over Europe, the new SOC formation approach applied here is not able to reproduce measured OC aerosol concentrations during winter. Many indications point to underestimated amounts from residential wood burning in large parts of Europe (e.g. Bergstroem et al., 2012; Langmann et al., 2008; Gelencser et al., 2007; Szidat et al., 2007). Updated emission inventories need to take into account the changing heating practices in Europe and the use of wood burning not only in rural but also in urban areas.

Supplementary material related to this article is available online at http://www.atmos-chem-phys-discuss.net/13/26761/2013/ acpd-13-26761-2013-supplement.pdf.

References

Allan, J. D., Delia, A. E., Coe, H., Bower, K. N., Alfarra, M. R., Jimenez, J. L., Middlebrook, A. M., Drewnick, F., Onasch, T. B., Canagaratna, M. R., Jayne, J. T., and Worsnop, D. R.: A generalised method for the extraction of chemically resolved mass spectra from aerodyne aerosol mass spectrometer data, J. Aerosol Sci., 35, 909–922, 2004.

Anttila, T., Langmann, B., Varghese, S., and O'Dowd, C.: Contribution of isoprene oxidation products to marine aerosol over the North-East Atlantic, Adv. Meteorol., 2010, 482603, doi:10.1155/2010/482603, 2010.

Canagaratna, M. R., Jayne, J. T., Jimenez, J. L., Allan, J. D., Alfarra, M. R., Zhang, Q., Onasch, T. B., Drewnick, F., Coe, H., Middlebrook, A., Delia, A., Williams, L. R., Trimborn, A. M., Northway, M. J., DeCarlo, P. F., Kolb, C. E., Davidovits, P., and Worsnop, D. R.:

Chemical and microphysical characterization of ambient aerosols with the aerodyne aerosol mass spectrometer, Mass Spectrometer Reviews, 26, 185–222, 2007.

Drewnick, F., Hings, S. S., DeCarlo, P., Jayne, J. T., Gonin, M., Fuhrer, K., Weimer, S., Jimenez, J. L., Demerjian, K. L., Borrmann, S., and Worsnop, D. R.: A new time-of-flight aerosol mass spectrometer (TOF-AMS)-instrument description and first field deployment, Aerosol Sci. Tech., 39, 637–658, 2005.

Ervens, B., Turpin, B. J., and Weber, R. J.: Secondary organic aerosol formation in cloud droplets and aqueous particles (aqSOA): a review of laboratory, field and model studies, Atmos. Chem. Phys., 11, 11069–11102, doi:10.5194/acp-11-11069-2011, 2011.

Freney, E. J., Sellegri, K., Canonaco, F., Boulon, J., Hervo, M., Weigel, R., Pichon, J. M., Colomb, A., Prévôt, A. S. H., and Laj, P.: Seasonal variations in aerosol particle composition at the puy-de-Dôme research station in France, Atmos. Chem. Phys., 11, 13047–13059, doi:10.5194/acp-11-13047-2011, 2011.

Fiedler, V., Dal Maso, M., Boy, M., Aufmhoff, H., Hoffmann, J., Schuck, T., Birmili, W., Hanke, M., Uecker, J., Arnold, F., and Kulmala, M.: The contribution of sulphuric acid to atmospheric particle formation and growth: a comparison between boundary layers in Northern and Central Europe, Atmos. Chem. Phys., 5, 1773–1785, doi:10.5194/acp-5-1773-2005, 2005.

Gantt, B., Meskhidze, N., Facchini, M. C., Rinaldi, M., Ceburnis, D., and O'Dowd, C. D.: Wind speed dependent size-resolved parameterization for the organic mass fraction of sea spray aerosol, Atmos. Chem. Phys., 11, 8777–8790, doi:10.5194/acp-11-8777-2011, 2011.

Gelencser, A., May, B., Simpson, D., Sanchez-Ochoa, A., Kasper-Giebl, A., Puxbaum, H., Caseiro, A., Pio, C., and Legrand, M.: Source apportionment of $PM_{2.5}$ organic aerosol over Europe: primary/secondary, natural/anthropogenic, fossil/biogenic origin, J. Geophys. Res., 112, D23S04, doi:10.1029/2006JD008094, 2007.

Griffin, R. J., Dabdub, D., and Seinfeld, J. H.: Secondary organic aerosol, I. Atmospheric chemical mechanism for production of molecular constituents, J. Geophys. Res., 107, 4332, doi:10.1029/2001JD000541, 2002.

Guenther, A. B., Monson, R. K., and Fall, R.: Isoprene and monoterpene emission rate variability: observations with eucalyptus and emission rate algorithm development, J. Geophys. Res., 96, 10799–10808, 1991.

Guenther, A. B., Zimmermann, P. R., Harley, P. C., Monson, R. K., and Fall, R.: Isoprene and monoterpene emission rate variability: model evaluation and sensitivity analysis, J. Geophys. Res., 98, 12609–12617, 1993.

Title Page

Abstract | Introduction

Conclusions | References

Tables | Figures

◄ | ►

◄ | ►

Back | Close

Full Screen / Esc

Printer-friendly Version

Interactive Discussion

Hallquist, M., Wenger, J. C., Baltensperger, U., Rudich, Y., Simpson, D., Claeys, M., Dommen, J., Donahue, N. M., George, C., Goldstein, A. H., Hamilton, J. F., Herrmann, H., Hoffmann, T., Iinuma, Y., Jang, M., Jenkin, M. E., Jimenez, J. L., Kiendler-Scharr, A., Maenhaut, W., McFiggans, G., Mentel, Th. F., Monod, A., Prévôt, A. S. H., Seinfeld, J. H., Surratt, J. D., Szmigielski, R., and Wildt, J.: The formation, properties and impact of secondary organic aerosol: current and emerging issues, Atmos. Chem. Phys., 9, 5155–5236, doi:10.5194/acp-9-5155-2009, 2009.

Hamed, A., Birmili, W., Joutsensaari, J., Mikkonen, S., Asmi, A., Wehner, B., Spindler, G., Jaatinen, A., Wiedensohler, A., Korhonen, H., Lehtinen, K. E. J., and Laaksonen, A.: Changes in the production rate of secondary aerosol particles in Central Europe in view of decreasing SO_2 emissions between 1996 and 2006, Atmos. Chem. Phys., 10, 1071–1091, doi:10.5194/acp-10-1071-2010, 2010.

Heald, C. L., Jacob, D. J., Park, R. J., Russell, L. M., Hubert, B. J., Seinfeld, J. H., Liao, H., and Weber, R. J.: A large organic aerosol source in the free troposphere missing from current models, Geophys. Res. Lett., 32, L18809, doi:10.1029/2005GL023831, 2005.

Henne, S., Brunner, D., Folini, D., Solberg, S., Klausen, J., and Buchmann, B.: Assessment of parameters describing representativeness of air quality in-situ measurement sites, Atmos. Chem. Phys., 10, 3561–3581, doi:10.5194/acp-10-3561-2010, 2010.

Henze, D. K. and Seinfeld, J. H.: Global secondary organic aerosol from isoprene oxidation, Geophys. Res. Lett., 33, L09812, doi:10.1029/2006GL025976, 2006.

Hodzic, A., Jimenez, J. L., Madronich, S., Canagaratna, M. R., DeCarlo, P. F., Kleinman, L., and Fast, J.: Modeling organic aerosols in a megacity: potential contribution of semi-volatile and intermediate volatility primary organic compounds to secondary organic aerosol formation, Atmos. Chem. Phys., 10, 5491–5514, doi:10.5194/acp-10-5491-2010, 2010.

Jimenez, J. L., Canagaratna, M. R., Donahue, N. M., Prevot, A. S. H., Zhang, Q., Kroll, J. H., DeCarlo, P. F., Allan, J. D., Coe, H., Ng, N. L., Aiken, A. C., Docherty, K. S., Ulbrich, I. M., Grieshop, A. P., Robinson, A. L., Duplissy, J., Smith, J. D., Wilson, K. R., Lanz, V. A., Hueglin, C., Sun, Y. L., Tian, J., Laaksonen, A., Raatikainen, T., Rautiainen, J., Vaattovaara, P., Ehn, M., Kulmala, M., Tomlinson, J. M., Collins, D. R., Cubison, M. J., Dunlea, E. J., Huffman, J. A., Onasch, T. B., Alfarra, M. R., Williams, P. I., Bower, K., Kondo, Y., Schneider, J., Drewnick, F., Borrmann, S., Weimer, S., Demerjian, K., Salcedo, D., Cottrell, L., Griffin, R., Takami, A., Miyoshi, T., Hatakeyama, S., Shimono, A., Sun, Y., Zhang, Y. M., Dzepina, K., Kimmel, J. R., Sueper, D., Jayne, J. T., Herndon, S. C., Trimborn, A. M., Williams, L. R., Wood, E. C.,

Middlebrook, A. M., Kolb, C. E., Baltensperger, U., and Worsnop, D. R.: Evolution of organic aerosols in the atmosphere, Science, 326, 1525–1529, 2009.

Kasper-Giebl, A., Koch, A., Hitzenberger, R., and Puxbaum, H.: Scavenging efficiency of aerosol carbon and sulfate in super-cooled clouds at Mt. Sonnblick (3106 m a.s.l., Austria), J. Atmos. Chem., 35, 33–46, 2000.

Kerminen, V.-M., Petäjä, T., Manninen, H. E., Paasonen, P., Nieminen, T., Sipilä, M., Junninen, H., Ehn, M., Gagné, S., Laakso, L., Riipinen, I., Vehkamäki, H., Kurten, T., Ortega, I. K., Dal Maso, M., Brus, D., Hyvärinen, A., Lihavainen, H., Leppä, J., Lehtinen, K. E. J., Mirme, A., Mirme, S., Hõrrak, U., Berndt, T., Stratmann, F., Birmili, W., Wiedensohler, A., Metzger, A., Dommen, J., Baltensperger, U., Kiendler-Scharr, A., Mentel, T. F., Wildt, J., Winkler, P. M., Wagner, P. E., Petzold, A., Minikin, A., Plass-Dülmer, C., Pöschl, U., Laaksonen, A., and Kulmala, M.: Atmospheric nucleation: highlights of the EUCAARI project and future directions, Atmos. Chem. Phys., 10, 10829–10848, doi:10.5194/acp-10-10829-2010, 2010.

Kroll, J. H. and Seinfeld, J. H.: Chemistry of secondary organic aerosol: formation and evolution of low-volatility organics in the atmosphere, Atmos. Environ., 42, 3593–3624, 2008.

Langmann, B.: Numerical modeling of regional scale transport and photochemistry directly together with meteorological processes, Atmos. Environ., 34, 3585–3598, 2000.

Langmann, B., Bauer, S. E., and Bey, I.: The influence of the global photochemical composition of the troposphere on European summer smog, Part I: Application of a global to mesoscale model chain, J. Geophys. Res., 108, 4146, doi:10.1029/2002JD002072, 2003.

Langmann, B., Varghese, S., Marmer, E., Vignati, E., Wilson, J., Stier, P., and O'Dowd, C.: Aerosol distribution over Europe: a model evaluation study with detailed aerosol microphysics, Atmos. Chem. Phys., 8, 1591–1607, doi:10.5194/acp-8-1591-2008, 2008.

Madronich, S.: Photodissociation in the atmosphere. 1. Actinic flux and the effect of ground reflections and clouds, J. Geophys. Res., 92, 9740–9752, 1987.

Majewski, D.: The Europa Modell of the Deutscher Wetterdienst, Seminar Proceedings ECMWF, vol. 2, 147–191, 1991.

Marmer, E. and Langmann, B.: Aerosol modelling over Europe Part I: Inter-annual variability of aerosol distribution, J. Geophys. Res., 112, D23S15, doi:10.1029/2006JD008113, 2007.

Mellor, B. and Yamada, T.: A hierarchy of turbulence closure models for planetary boundary layers, J. Atmos. Sci., 31, 1791–1806, 1974.

Metzger, A., Verheggen, B., Dommen, J., Duplissy, J., Prevot, A. S. H., Weingartner, E., Riipinen, I., Kulmala, M., Spracklen, D. V., Carslaw, K. S., and Baltensperger, U.: Evidence for

Secondary organic aerosol formation during June 2010 in Central Europe

B. Langmann et al.

Title Page

Abstract | Introduction

Conclusions | References

Tables | Figures

◀ | ▶

◀ | ▶

Back | Close

Full Screen / Esc

Printer-friendly Version

Interactive Discussion

the role of organics in aerosol particle formation under atmospheric conditions, P. Natl. Acad. Sci. USA, 107, 6646–6651, 2010.

O'Dowd, C., Langmann, B., Varghese, S., Scannell, C., Ceburnis, D., and Facchini, M. C.: A combined organic–inorganic sea-spray source function, Geophys. Res. Lett., 35, L01801, doi:10.1029/2007GL030331, 2008.

Odum, J. R., Hoffmann, T., Bowman, F., Collins, D., Flagan, R. C., and Seinfeld, J. H.: Gas/particle partitioning and secondary organic aerosol yields, Environ. Sci. Technol., 30, 2580–2585, 1996.

Ovadnevaite, J., Ceburnis, D., Canagaratna, M., Berresheim, H., Bialek, J., Mrtucci, G., Worsnop, D. R., and O'Dowd, C.: On the effect of wind speed on submicron sea salt mass concentration and source fluxes, J. Geophys. Res. 117, D16201, doi:10.1029/2011JD017379, 2012.

Paasonen, P., Nieminen, T., Asmi, E., Manninen, H. E., Petäjä, T., Plass-Dülmer, C., Flentje, H., Birmili, W., Wiedensohler, A., Hõrrak, U., Metzger, A., Hamed, A., Laaksonen, A., Facchini, M. C., Kerminen, V.-M., and Kulmala, M.: On the roles of sulphuric acid and low-volatility organic vapours in the initial steps of atmospheric new particle formation, Atmos. Chem. Phys., 10, 11223–11242, doi:10.5194/acp-10-11223-2010, 2010.

Pankow, J. F.: An absorption model of the gas/aerosol partitioning involved in the formation of secondary organic aerosol, Atmos. Environ., 28, 189–193, 1994.

Roeckner, E., Arpe, K., Bengtsson, L., Christoph, M., Claussen, M., Dümenil, L., Esch, M., Giorgetta, M., Schlese, U., and Schulzweida, U.: The atmospheric general circulation model ECHAM-4: Model description and simulation of present-day climate, MPI-Report No. 218, Max Planck Institute for Meteorology, Hamburg, Germany, 1996.

Saxena, P. and Hildemann, L. M.: Water-soluble organics in atmospheric particles: a critical review of the literature and application of thermodynamics to identify candidate compounds, J. Atmos. Chem., 24, 57–109, 1996.

Shrivastava, M., Fast, J., Easter, R., Gustafson Jr., W. I., Zaveri, R. A., Jimenez, J. L., Saide, P., and Hodzic, A.: Modeling organic aerosols in a megacity: comparison of simple and complex representations of the volatility basis set approach, Atmos. Chem. Phys., 11, 6639–6662, doi:10.5194/acp-11-6639-2011, 2011.

Smolarkiewitz, P. K.: A simple positive definite advection scheme with small implicit diffusion, Mon. Weather Rev., 111, 479–486, 1983.

Stier, P., Feichter, J., Kinne, S., Kloster, S., Vignati, E., Wilson, J., Ganzeveld, L., Tegen, I., Werner, M., Balkanski, Y., Schulz, M., Boucher, O., Minikin, A., and Petzold, A.: The aerosol-climate model ECHAM5-HAM, Atmos. Chem. Phys., 5, 1125–1156, doi:10.5194/acp-5-1125-2005, 2005.

Stockwell, W. R., Middleton, P., Chang, J. S., and Tang, X.: The second generation regional acid deposition model: chemical mechanism for regional air quality modelling, J. Geophys. Res., 95, 16343–16367, 1990.

Szegvary, T., Conen, F., and Ciais, P.: European 222Rn inventory for applied atmospheric studies, Atmos. Environ., 43, 1536–1539, 2009.

Szidat, S., Prevot, A. S. H., Sandradewi, J., Sandradewi, J., Alfarra, M. R., Synal, H.-A., Wacker, L., and Baltensperger, U.: Dominant impact of residential wood burning on particulate matter in Alpine valleys during winter, Geophys. Res. Lett., 34, L05820, doi:10.1029/2006GL028325, 2007.

Tiedtke, M.: A comprehensive mass flux scheme for cumulus parameterisation in large-scale models, Mon. Weather Rev., 117, 1778–1800, 1989.

Vehkamaeki, H., Kumala, M., Napari, I., Lehtinen, K. E. J., Timmreck, C., Noppel, M., and Laaksonen, A.: An improved parameterization for sulphuric acid-water nucleation rates for tropospheric and stratospheric conditions, J. Geophys. Res., 107, 4622, doi:10.1029/2002JD002184, 2002.

Venzac, H., Sellegri, K., Villani, P., Picard, D., and Laj, P.: Seasonal variation of aerosol size distributions in the free troposphere and residual layer at the puy de Dôme station, France, Atmos. Chem. Phys., 9, 1465–1478, doi:10.5194/acp-9-1465-2009, 2009.

Vignati, E., Wilson, J., and Stier, P.: M7, an efficient size-resolved aerosol microphysics module for large-scale aerosol transport models, J. Geophys. Res., 109, D22202, doi:10.1029/2003JD004485, 2004.

Walcek, C. J. and Taylor, G. R.: A theoretical method for computing vertical distributions of acidity and sulfate production within cumulus clouds, J. Atmos. Sci., 43, 339–355, 1986.

Walcek, C. J., Brost, R. A., Chang, J. S., and Wesley, M. L.: SO_2, Sulfate and HNO_3 deposition velocities computed using regional landuse and meteorological data, Atmos. Environ., 20, 946–964, 1986.

Wesley, M. L.: Parameterization of surface resistances to gaseous dry deposition in regional-sclae numerical models, Atmos. Environ., 23, 1293–1304, 1989.

|◄ | ►|

◄ | ►

Back | Close

Full Screen / Esc

Printer-friendly Version

Interactive Discussion

Yu, F.: A secondary organic aerosol formation model considering successive oxidation aging and kinetic condensation of organic compounds: global scale implications, Atmos. Chem. Phys., 11, 1083–1099, doi:10.5194/acp-11-1083-2011, 2011.

Zhang, K., Feichter, J., Kazil, J., Wan, H., Zhuo, W., Griffiths, A. D., Sartorius, H., Zahorowski, W., Ramonet, M., Schmidt, M., Yver, C., Neubert, R. E. M., and Brunke, E.-G.: Radon activity in the lower troposphere and its impact on ionization rate: a global estimate using different radon emissions, Atmos. Chem. Phys., 11, 7817–7838, doi:10.5194/acp-11-7817-2011, 2011.

Secondary organic aerosol formation during June 2010 in Central Europe

B. Langmann et al.

Table 1. Properties of medium- and semi-volatile secondary gases (MV-SOG and SV-SOG) based on Anttila et al. (2010). Note, that the Henry Law coefficient for MV-SOG has been increased by one order of magnitude.

Compound	Stoichiometric coefficients	Molecular weight ($g\,mol^{-1}$)	K_H 298 K ($M\,atm^{-1}$)
MV-SOG	0.28	76.1	9.1×10^{6}
SV-SOG	0.032	106.0	3×10^{11}
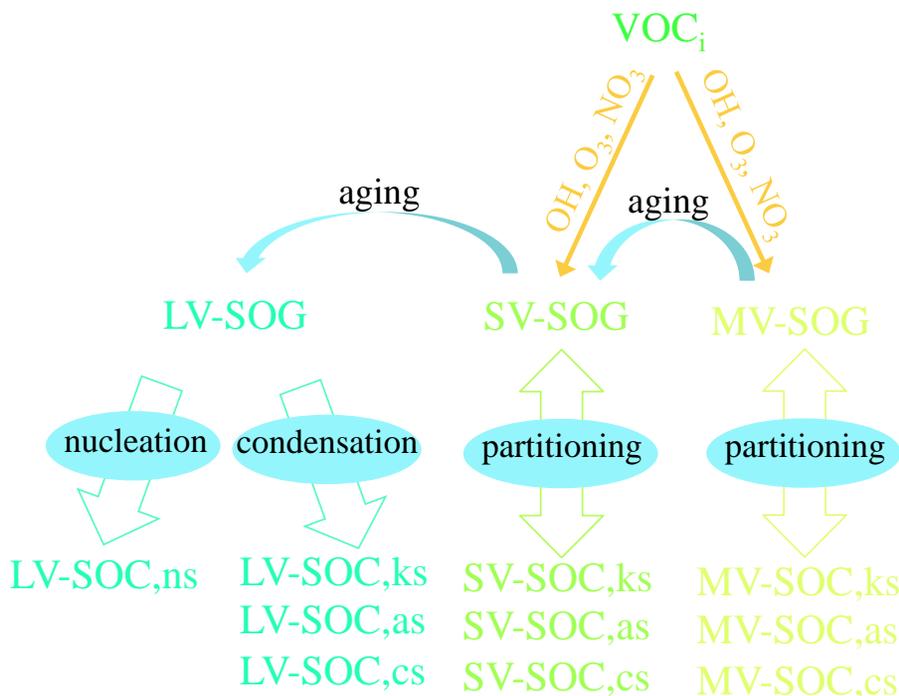
Fig. 1. Schematic illustration of SOC particle formation and oxidation aging processes. VOC_i: precursor gases, SOG: secondary organic gas, SOC: secondary organic carbon aerosol, LV: low volatile, SV: semi volatile, MV: medium volatile, ns: nucleation mode soluble, ks: aitken mode soluble, as: accumulation mode soluble, cs: coarse mode soluble.

Title Page

Abstract | Introduction

Conclusions | References

Tables | Figures

|◄ | ►|

◄ | ►

Back | Close

Full Screen / Esc

Printer-friendly Version

Interactive Discussion
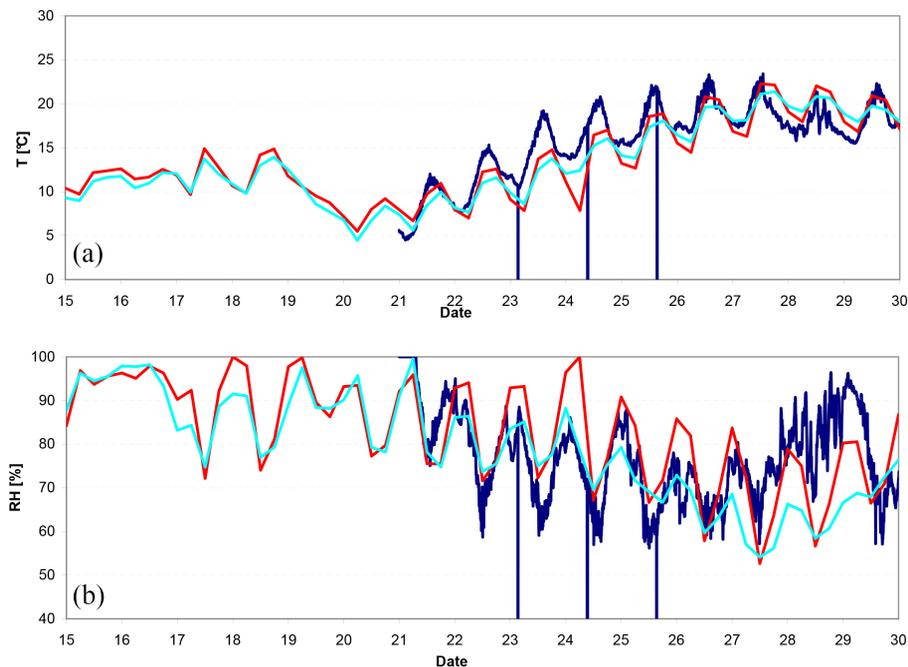
Fig. 2. Meteorological situation at Puy-de-Dôme during June 2010. **(a)** Temperature [°C], **(b)** relative humidity [%]. Dark blue line: measurements, red line: model results first layer, light blue line: model results second layer.

Secondary organic aerosol formation during June 2010 in Central Europe

B. Langmann et al.

Title Page

Abstract | Introduction

Conclusions | References

Tables | Figures

◀ | ▶

◀ | ▶

Back | Close

Full Screen / Esc

Printer-friendly Version

Interactive Discussion
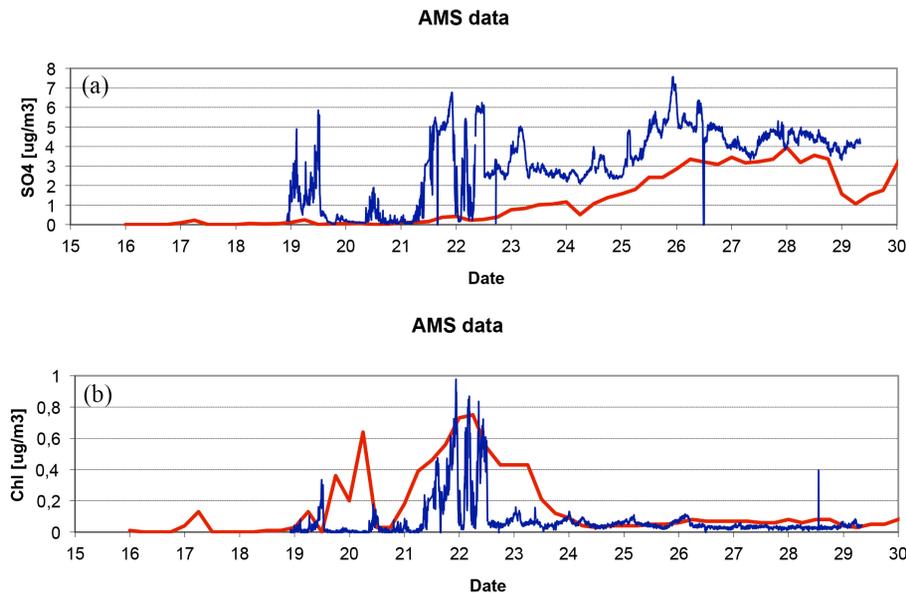
Fig. 3. AMS-measured (dark blue line) and modelled (red line) near surface aerosol mass concentration during June 2010 at Puy-de-Dôme, France. **(a)** Sulfate [$\mu g\,m^{-3}$], **(b)** Chlorine [$\mu g\,m^{-3}$].
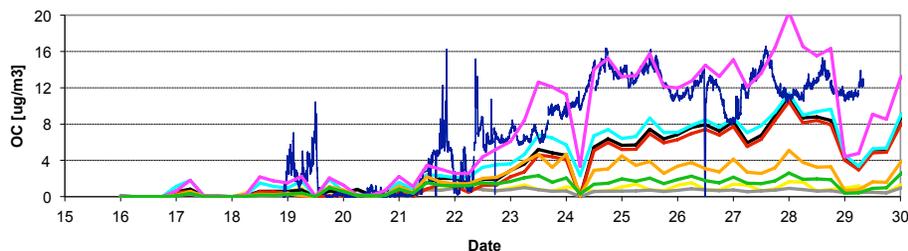
Fig. 4. AMS-measured (dark blue line) and modelled near surface SOC mass concentration during June 2010 at Puy-de-Dôme, France. Grey line: according to Anttila et al. (2010); yellow line: more VOC precursor gases; green line: SOG transport and removal; orange line: SOG transport and removal plus biogenic emissions × 5; red line: 1. aging SOG – 1 % aging; black line: 2. aging SOG – 1 % aging, light blue line: 2. aging SOG – 10 % aging; magneta line: 2. aging SOG – 10 % aging plus biogenic emissions × 5. See text for more explanation.
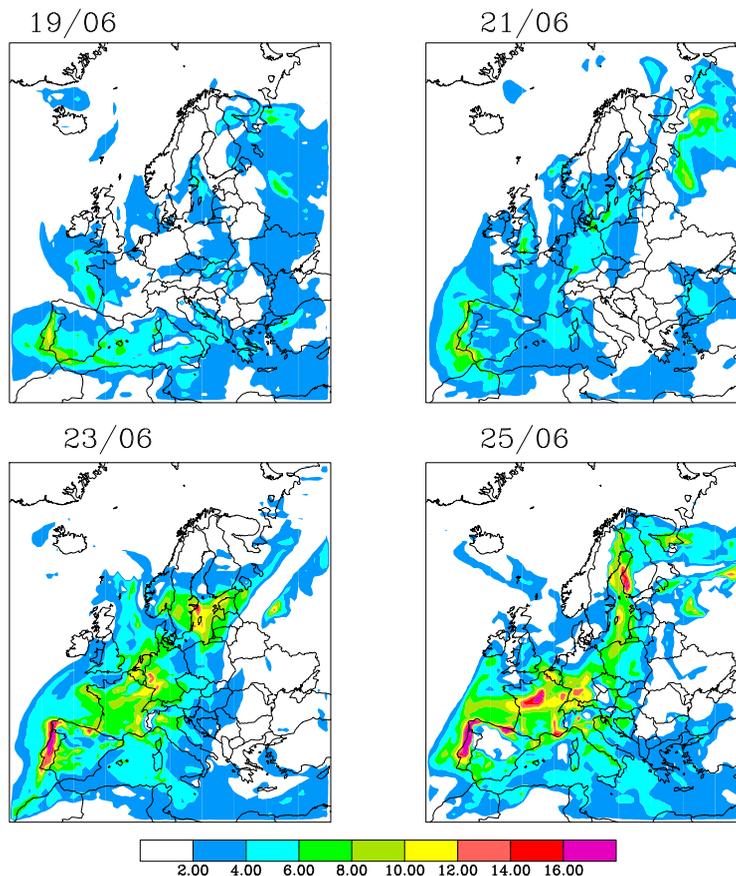
Fig. 5. Modelled near surface concentration of organic carbon aerosol in $\mu g\,m^{-3}$ on 19, 21, 23 and 25 June at 18:00 UTC by considering the second aging of SOG gas and a threshold of 10 % for aging. Model simulation results correspond to those shown as light blue line in Fig. 4.
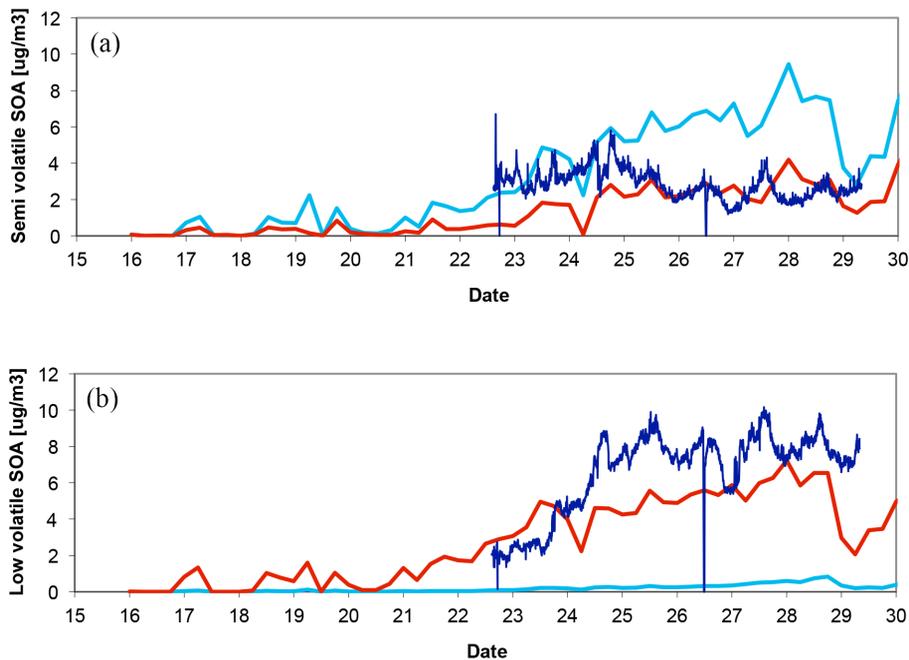
Fig. 6. Volatility of SOC near surface aerosol mass concentration during June 2010 at Puy-de-Dôme, France. **(a)** Semi volatile SOC, **(b)** low volatile SOC. Dark blue line: AMS-measured, light blue line: 2. aging SOG – 1 % aging, red line: 2. aging SOG – 10 % aging. Model simulation results correspond to those shown as light blue line in Fig. 4.
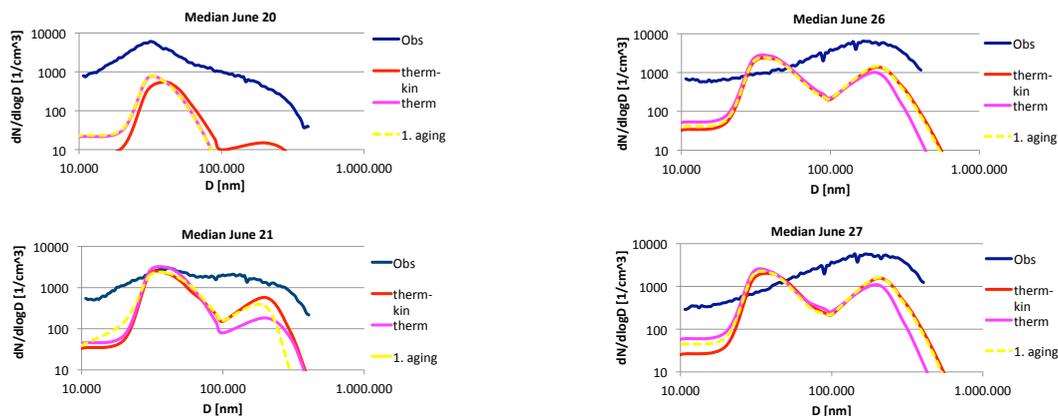
Fig. 7. Median dry aerosol number size-distribution [cm^{-3}] at Puy-de-Dôme for fresh air masses (20 and 21 June) and aged air masses (26 and 27 June). Blue line: measured median; red line: modelled daytime median with thermodynamic-kinetic approach; magneta line: modelled daytime median with pure thermodynamic approach; yellow line: modelled daytime median with first aging step only.
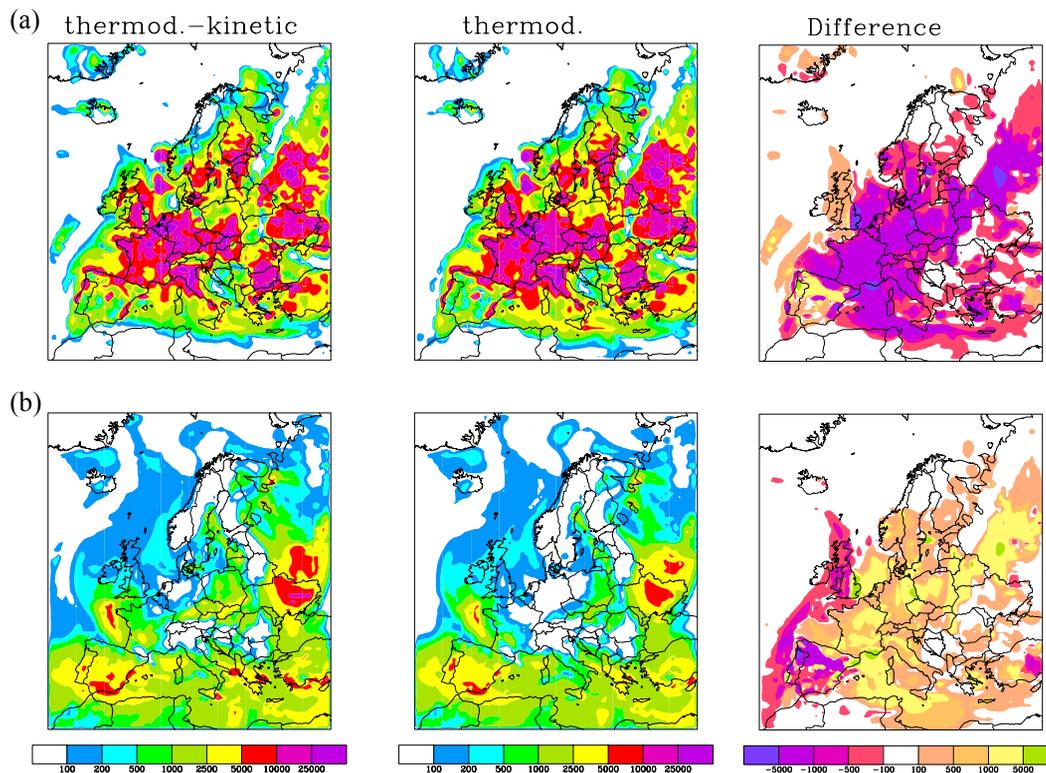
Fig. 8. Modelled near surface particle number concentration [cm^{-3}] in **(a)** the aitken and **(b)** the accumulation mode on 22.06.2010, 18:00 UTC over Europe. The difference is determined by subtraction of the thermodynamic data from the mixed thermodynamic-kinetic data.

Title Page

Abstract | Introduction

Conclusions | References

Tables | Figures

|◄ | ►|

◄ | ►

Back | Close

Full Screen / Esc

Printer-friendly Version

Interactive Discussion
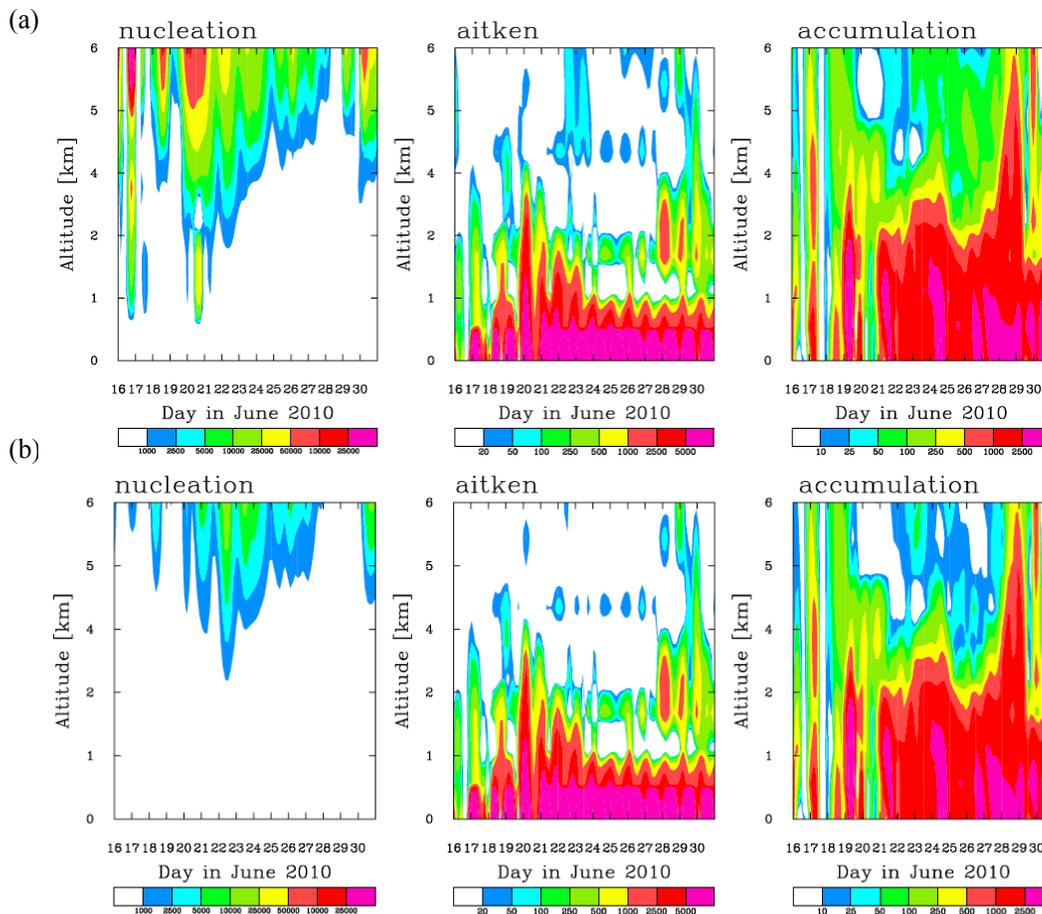
Fig. 9. Modeled vertical profiles of particle number concentration in the nucleation (left column), aitken (middle column) and accumulation mode (right column) at Puy-de-Dôme in cm^{-3} during June 2010 **(a)** with LV-SOG nucleation and **(b)** without LV-SOG nucleation.

Title Page

Abstract | Introduction

Conclusions | References

Tables | Figures

|◄ | ►|

◄ | ►

Back | Close

Full Screen / Esc

Printer-friendly Version

Interactive Discussion